Hypericin Activates L-Type Ca^{2+} Channels in Cardiac Myocytes

Martin-Pierre Sauviat,*,[†] Anthony Colas,[†] Marie-Jeanne Chauveau,[‡] Jean-Claude Drapier,[‡] and Michel Négrerie[†]

Laboratoire d'Optique et Biosciences, U696 INSERM, UMR7645 CNRS, X/ENSTA, Ecole Polytechnique, Route de Saclay, 91128 Palaiseau Cedex, France, and Institut de Chimie des Substances Naturelles, CNRS, Bâtiment 27, Avenue de la Terrasse, 91198 Gif-sur-Yvette Cedex, France

The effects and the mode of action of hypericin (**1**) were studied, in the dark, on the action potential (AP) and the L-type Ca^{2+} channel of frog atrial heart muscle, using intracellular microelectrode and patch-clamp techniques, respectively. In the presence of Ca^{2+} in Ringer solution, hypericin (1 to 4 μM) did not markedly modify the AP. Total replacement of Ca^{2+} by Sr^{2+} in the solution (Ringer Sr^{2+}) revealed that hypericin (4 μM) prolonged the AP duration (APD). Hypericin dose-dependently increased the magnitude of the Sr^{2+}current, which develops through L-type Ca^{2+} channels in the Ringer solution containing tetrodotoxin (0.7 μM) and tetraethylammonium (10 mM), but did not modify the kinetics of activation and inactivation. This revealed that hypericin increased L-type Ca^{2+} channel conductance, which accounted for the APD lengthening. The hypericin-induced APD lengthening recorded in the Ringer Sr^{2+} was not prevented by (i) a blockade of α- and β-adrenoceptors by yohimbine (1 μM), urapidil (1 μM), and propanolol (50 μM), respectively, and (ii) PKC blockade by staurosporine (1 μM). The hypericin-induced APD lengthening recorded in the Ringer Sr^{2+} was prevented by blocking soluble guanylate cyclase (sGC) activity by 1*H*-[1,2,4]-oxadiazolo[4,3-*a*]quinoxalin-1-one (13 μM), which mimicked the effects of hypericin. Hypericin decreased the cellular cGMP level by 69% in atrial myocytes. The compound also decreased the cellular cGMP level by inhibiting sGC, thus cancelling the nucleotide inhibitory effect on the cardiac L-type Ca^{2+} channel.

St. John's Wort extract (*Hypericum perforatum* L.) (Hypericaceae), for which various healing virtues have been attributed since antiquity, is used as an antidepressant in phytomedicine.[1,2] Hypericin (**1**) and hyperforin are the main bioactive substances present in this extract. Hypericin is a lipophilic natural photoactivable red pigment that belongs to the naphthodianthrone family (Figure 1), and is responsible for the solar syndrome that affects cattle after ingestion of large amounts of St. John's Wort.[1] The molecule incorporates in membrane phospholipid bilayers, penetrates into the cells,[3] and concentrates in the perinuclear cytoplasm area of the nucleus, corresponding to the endoplasmic reticulum and Golgi apparatus.[4] Previous studies have reported that an extract of St. John's Wort did not affect heart-rate variability[5] and that hypericin (20 μM) did not alter the contraction of guinea-pig ventricular papillary muscle.[6] Since little is known about the cardiac effects of **1**, the goal of the present work was to study the effects and the mode of action of **1** in the dark, because of the photoactivation of the molecule,[2] on the electrical activity of the cardiac membrane.

Results and Discussion

The addition of hypericin (**1**, 4 μM) to the Ringer solution used did not change the time-course of the action potential (AP) of spontaneously beating auricles (Figure 2A). Increasing the concentration of **1** from 1 to 4 μM in the Ringer solution did not significantly modify the resting membrane potential (RP), overshoot (OS), and the AP duration (APD) (Table 1). Total replacement of Ca^{2+} by Sr^{2+} in the Ringer solution (Ringer Sr^{2+}) markedly increased the plateau duration (APD$_0$ and APD$_{40}$) and prolonged the AP repolarization phase APD$_{10}$ (Figure 2B). Table 1 shows that the APD$_0$, APD$_{40}$, and APD$_{10}$ were markedly prolonged in the Ringer Sr^{2+}solution compared to the Ringer Ca^{2+} solution. Subsequent addition of hypericin (**1**, 4 μM) to the Ringer Sr^{2+} solution led to an extra lengthening of the plateau and phase of repolarization (Figure 2B). Table 1 shows that **1** significantly ($p > 0.05$) lengthened APD$_0$ (26%), APD$_{40}$ (22%), and APD$_{10}$ (39%).

* To whom correspondence should be addressed. Tel: (33) 01 69 33 50 57. Fax: (33) 01 69 31 97 71. E-mail: martin-pierre.sauviat@polytechnique.edu.
[†] Laboratoire d'Optique et Biosciences.
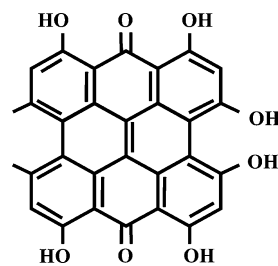[‡] Institut de Chimie des Substances Naturelles.

Figure 1. Structural formula of hypericin (**1**),[1] a polycyclic aromatic 2,2′-dimethyl-4,4′,5,5′,7,7′-hexahydroxy-*meso*-naphthodianthrone.
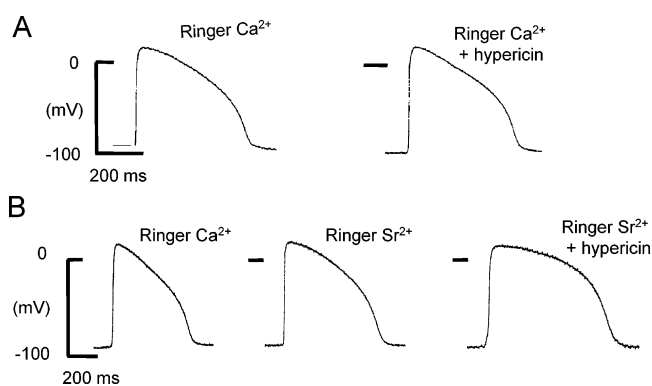

Figure 2. Effects of hypericin (**1**) on the spontaneously beating action potential (AP) of frog atrial heart muscle. (A). Typical AP recorded on the same auricle in Ringer solution containing 2 mM Ca^{2+} (Ringer Ca^{2+}) before and 5 min after hypericin (**1**, 4 μM) application. (B). AP traces recorded successively on the same auricle in (left trace) Ringer Ca^{2+}; (middle trace) Ca^{2+}-free Ringer solution containing Sr^{2+} (2 mM; Ringer Sr^{2+}); and (right trace) Ringer Sr^{2+} containing hypericin (**1**, 4 μM) for 5 min.

$I_{\text{Sr(L)}}$ recorded from voltage-clamped myocytes bathed in a Ringer Sr^{2+} solution containing tetrodotoxin (TTX) (0.7 μM) and tetraethylammonium (TEA) (10 mM) remained inward more than 500 ms after the onset of the depolarizing step (Figure 3A). Subsequent addition of hypericin (**1**, 4 μM) to the control solution increased

Table 1. Effects of Hypericin (**1**) on Frog Atrial AP[a,b]

treatment	RP (mV)	OS (mV)	APD_0 (ms)	APD_{40} (ms)	APD_{10} (ms)
(A)					
Ringer Ca^{2+}	-92.3 ± 0.8	19.5 ± 0.5	160.2 ± 3.6	408.2 ± 5.0	471.4 ± 4.4
hypericin (**1**) 1 μM	-94.0 ± 0.8	19.3 ± 0.4	156.1 ± 4.4	402.2 ± 3.0	464.2 ± 3.2
hypericin (**1**) 2 μM	-94.1 ± 0.6	19.5 ± 0.5	165.2 ± 4.7	412.1 ± 2.8	469.3 ± 7.1
hypericin (**1**) 4 μM	-94.3 ± 0.6	19.3 ± 0.4	171.0 ± 4.3	419.5 ± 2.5	471.6 ± 3.0
(B)					
Ringer Sr^{2+}	-85.4 ± 0.9	17.6 ± 0.5	528 ± 10	600 ± 9	708 ± 10
hypericin (**1**) 4 μM	-84.5 ± 0.8	17.6 ± 0.5	665 ± 10^c	729 ± 10^c	981 ± 14^c

[a] AP were recorded (A) in the presence of Ca^{2+} (2 mM; Ringer Ca^{2+}) and (B) in a Ca^{2+}-free solution containing Sr^{2+} (2 mM; Ringer Sr^{2+}). [b] RP = resting membrane potential; OS = amplitude of the overshoot; APD_0 = duration of the AP measured at 0 mV; APD_{40} and APD_{10} = duration of the AP measured at a membrane potential +40 and +10 mV higher than RP, respectively. The data are means $\pm$ SD of 6 auricles. [c] $p > 0.05$, hypericin (**1**) vs Ringer Sr^{2+}.
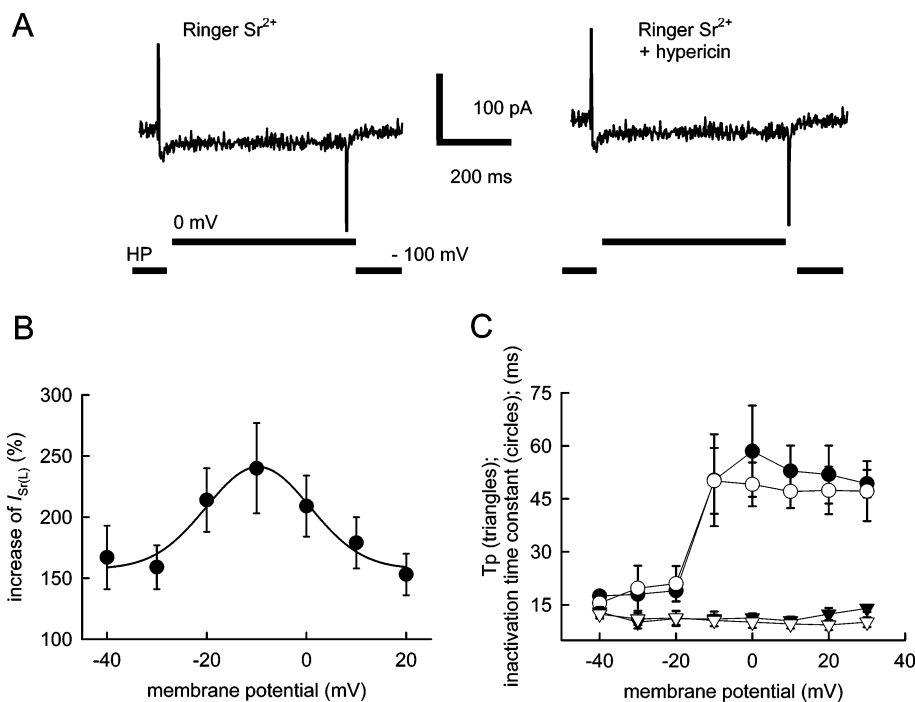

Figure 3. Effects of hypericin (**1**, 4 μM) on voltage-clamped atrial myocytes bathed in control Ringer Sr^{2+} containing TTX (0.7 μM) and TEA (10 mM). (A) Membrane inward Sr^{2+} current ($I_{Sr(L)}$) recorded during voltage steps to 0 mV from a HP of -100 mV (schematic beneath the traces) before and 5 min after hypericin addition to the control solution. (B) Hypericin-induced $I_{Sr(L)}$ increase as a function of membrane potential. The curve expresses the ratio (in percentage) of $I_{Sr(L)}$ amplitude mean values $\pm$ SD obtained on 7 cells before and after hypericin treatment as a function of the membrane potential. (C) Time to peak (Tp; triangles) and time constant of the inactivation phase (circles) of $I_{Sr(L)}$ as a function of the membrane potential: (open symbols) control solution; (filled symbols) control solution containing hypericin (**1**). Tp and time constant inactivation phase of $I_{Sr(L)}$ mean values $\pm$ SD obtained on 7 cells before and after hypericin treatment reported as a function of the membrane potential. A, B, and C: HP = -100 mV.

the amplitude of $I_{Sr(L)}$ within 5 min (Figure 3A). The **1**-induced increase in $I_{Sr(L)}$ amplitude occurred at all membrane potentials tested and followed a Gaussian distribution (Figure 3B). Current–voltage relationships plotted for $I_{Sr(L)}$ showed that in the presence of **1** (4 μM) $I_{Sr(L)}$ started to activate at a membrane potential of -69 ± 4 mV ($n = 7$) instead of -50 ± 5 mV ($n = 6$) in the absence of **1**, while the membrane potential at which $I_{Sr(L)}$ reached its maximum value (-6 ± 3 mV, $n = 7$) remained unchanged. Whatever the membrane potential investigated, hypericin (**1**) application modified neither the time to peak nor the time constant of the inactivation phase of $I_{Sr(L)}$ (Figure 3C). Figure 4 shows that the hypericin-induced increase in $I_{Sr(L)}$ magnitude was dose-dependent. The data showed that **1** increased L-type Ca^{2+} channel conductance. They also indicated that, in the Ringer Sr^{2+} solution, a change in APD reflects a change in $I_{Sr(L)}$. Consequently, AP recording was used in the experiments described below.

Regulation of L-type Ca^{2+} channels is complex and involves different pathways such as (i) the adrenergic pathway via AC activation and the cAMP cascade and (ii) the NO pathway via NOS and sGC activation and the cGMP cascade.

Blockade of α_1 and α_2 adrenoceptors by addition of urapidil (1 μM) and yohimbine (1 μM) and blockade of β_1 and β_2 adrenoceptors by addition of propanolol (50 μM) to the Ringer Sr^{2+} solution increased OS (14%) and prolonged APD_0 (41%), APD_{40} (33%), and APD_{10} (42%), as shown in Table 2. Subsequent addition of hypericin (**1**, 4 μM) to the solution containing α- and β-adrenoceptor blockers produced a significant ($p > 0.05$) extra-lengthening of APD_0 (25%), APD_{40} (16%), and APD_{10} (20%) (Table 2). Activation of adenylcyclase by addition of FSK (1 μM) to the Ringer Sr^{2+} solution significantly increased OS (20%) and prolonged APD_0 (28%), APD_{40} (4%), and APD_{10} (12%) (Table 2). Further addition of **1** (4 μM) to the Ringer Sr^{2+} containing FSK caused significant ($p > 0.05$) lengthening of only APD_{10} by 21% (Table 2). In the presence of staurosporine (1 μM) in the Ringer Sr^{2+} solution, to inhibit PKC, APD_0 (33%), APD_{40} (24%), and APD_{10} (30%) were prolonged considerably ($p > 0.05$) (Table 2). Staurosporine did not prevent the significant ($p > 0.05$) lengthening of APD_0 (6%), APD_{40} (11%), and APD_{10} (18%) produced by subsequent addition of hypericin (**1**, 4 μM) to the solution containing staurosporine
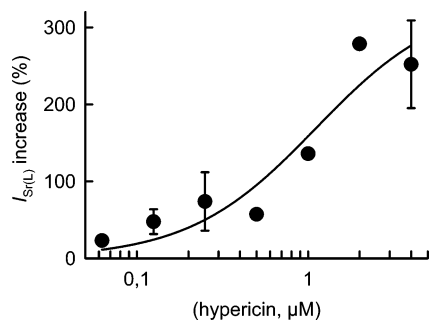
Figure 4. Dose−response curve for the increase of $I_{Sr(L)}$ induced by hypericin (**1**). Increase is expressed as % of the amplitude of $I_{Sr(L)}$ recorded at 0 mV (HP = −100 mV) in Ringer Sr^{2+} containing TTX (0.7 μM) and TEA (10 mM). The curve fitting through experimental data was drawn according the regression equation $Y = Y_{max} X/(K_d + X)$ where Y is the percentage of $I_{Sr(L)}$ inhibition; X the hypericin concentration; K_d the apparent dissociation constant; Y_{max} a constant value Y ($K_d = 1.56$ μM correlation coeficient = 0.99). Data are means ± SD of 6 cells.

(Table 2). The microscystin bioassay used reveals that hypericin (**1**) (0.4 to 40 μM) did not affect PP2A activity.

The addition of ODQ (13 μM) to the Ringer Sr^{2+} solution significantly ($p > 0.05$) lengthened APD_{40} (12%) and APD_{10} (21%), as shown in Table 3. Subsequent addition of hypericin (**1**, 4 μM) to the solution containing ODQ did not change the APD (Table 3). The addition of enterotoxin STa (10^{-6} U mL^{-1}) to the Ringer Sr^{2+} solution prolonged APD_{40} and APD_{10} significantly ($p > 0.05$) (Table 3), and the addition of ANF (6.5 μM) to the Ringer Sr^{2+} solution significantly ($p > 0.05$) prolonged APD_0, APD_{40}, and APD_{10} (Table 3). However, both substances did not prevent the extra ($p > 0.05$) APD lengthening produced by subsequent addition of hypericin (**1**, 4 μM) to the solutions containing these substances (Table 3).

Heme capture assay experiments showed that hypericin (**1**) in the concentration range 0.1 to 10 μM had no direct effect on the hemoglobin NOS2. The absolute measurement of the cellular cGMP content ([cGMP]) of atrial myocytes showed that it increased linearly with increasing volumes of the incubating solution (Figure 5) in the absence of **1**, while it was decreased markedly in the presence of the compound (4 μM) in the solution. [cGMP] was 1.259 fM in the absence and 0.386 fM in the presence of **1**, i.e., was reduced by 69% (Figure 5). Therefore, with an average weight of frog auricles of 29.6 ± 2.5 mg ($n = 3$), [cGMP] is 0.047.06 fM/mg in the absence and 0.013 fM/mg in the presence of hypericin (**1**, 4 μM).

The present results demonstrated that hypericin (**1**) increases the conductance of L-type Ca^{2+} channels by decreasing the [cGMP] in frog atrial heart muscle. Thus, hypericin (**1**) increased dose-dependently the conductance of L-type Ca^{2+} channels without affecting their kinetics of activation and inactivation. The data also showed that $I_{Sr(L)}$ increase could not be attributed to a sustained phosphorylation of the channel since hypericin did not affect PP2A activity as revealed by a microscystin bioassay. It is thus likely that $I_{Sr(L)}$ that inactivated slowly was responsible for the marked lengthening of the plateau and repolarizing phase of frog atrial tissue AP.[7,17] In the presence of Ca^{2+}, L-type Ca^{2+} channel conductance increase led to a faster inactivation of the Ca^{2+} current and to the triggering of Ca^{2+}-activated K$^+$ current and may account for the absence of a clear-cut effect of hypericin on the APD observed in the presence of Ca^{2+}.

The results clearly indicated that hypericin (**1**) lengthened the APD when α- and β-adrenoceptors previously had been blocked. However, they show that after previous AC activation by FSK prior treatment with **1**, the APD still increased in the presence of this substance, which suggested that the effects of FSK and **1** on the APD were additive. It is worth noting that direct AC activation by

FSK has been shown to raise evidence in favor of a phosphodi-esterase-2 (PDE2) inhibition of $I_{Ca(L)}$ by cGMP and/or NO donors in the frog ventricle.[18] The data also show that PKC blockade by staurosporine prolongs the APD but does not prevent the APD extra-lengthening induced by hypericin (**1**). Therefore, it may be concluded from these data that the L-type Ca^{2+} channel conductance increase induced by hypericin (**1**) is not a consequence of the direct activation of the cAMP pathway by this substance.

These results show that ODQ lengthened the APD and mimicked the effect of hypericin (**1**) and additionally prevented the develop-ment of hypericin-induced APD lengthening. ODQ specifically inhibits sGC activity by binding to heme and prevents NO binding, leading to a decrease of the intracellular cGMP level. ODQ increases $I_{Ca(L)}$ in guinea-pig cardiac myocytes.[19] In cat atrial myocytes, NO signaling mediates stimulation of $I_{Ca(L)}$ elicited by withdrawal of acetylcholine, and NO activates cGMP-induced inhibition of phosphodiesterase (type III) activity,[20] while cGMP inhibits $I_{Ca(L)}$ in guinea-pig ventricular myocytes.[21] In the present study, hypericin (**1**) markedly decreased the cellular level of cGMP in frog auricle myocytes. A reduction of [cGMP] removes PDE2 inhibition of L-type Ca^{2+} channels and increases the channel conductance. Therefore, it may be assumed that the decrease of [cGMP] produced by hypericin (**1**) is involved in $I_{Ca(L)}$ increase. These data show that [cGMP] affects physiological properties of the cardiac L-type Ca^{2+} channel. As a consequence of $I_{Ca(L)}$ increase, an increase in I_{K-Ca} and I_{K1} may develop, leading to insignificant effects on APD induced by hypericin (**1**) in the presence of Ca^{2+} in the control solution (see Table 1). The results also revealed that hypericin (**1**) did not affect NOS2. In addition, the blockade of transmembrane GC receptors by STa or by ANF did not prevent the APD lengthening induced by hypericin, indicating that **1** does not bind to these receptors. Taken together, these results reveal that hypericin (**1**) inhibits sGC.

Therefore, in conclusion, the present data demonstrate that hypericin (**1**) increased the conductance of frog cardiac L-type Ca^{2+} channels by modulating [cGMP] via an inhibition of sGC. To our knowledge, this is the first time that such direct evidence concerning L-type Ca^{2+} channels regulation via the cGMP pathway has been reported. Such a mechanism of action might be taken into account for the use of St. John's Wort extracts containing hypericin (**1**), as an antidepressant.

Experimental Section

Test Compound. High-purity hypericin (**1**) (Molecular Probes, Leiden, The Netherlands) was diluted in dimethylsulfoxide (DMSO) and was protected from light before and during the experiments. In control experiments, the addition of DMSO at a final concentration of 10 μM to the standard solution does not affect the AP and transmem-brane currents.

Animal Material. Electrophysiological experiments were performed in the dark at 19−20 °C on the whole auricle and on enzymatically isolated auricular myocytes obtained from the heart of the adult frog, *Rana esculenta*.

Electrophysiological Experiments. Transmembrane Potentials and Current Measurement. The resting potential (RP, i.e., the potential difference between the inside and the outside of the membrane at rest) and the action potential (AP, i.e., the transient change in membrane potential that represents the electrical envelope of the cascade of ionic movements through the membrane triggered by a stimulus) were recorded on the whole cleaned quiescent auricle. Glass micro-electrodes (filled with saturated KCl; 25−30 MΩ resistance; tip potential > ±3 mV) were used in the "floating" mode.[11] In the present study, were measured RP; the amplitude of the overshoot (OS); the AP duration (APD) at a membrane potential of (i) 0 mV (APD_0) and +40 mV higher than RP (APD_{40}) to estimate the variation of the plateau duration and (ii) +10 mV higher than RP (APD_{10}) to estimate the changes in the duration of membrane repolarization. Due to a possible difference between animals, 12 successive APs (RP ≥ −80 mV; OS ≥ +15 mV) were recorded in each solution tested, and the calculated

Table 2. Effects of Hypericin (**1**) on Frog Atrial AP under Various Conditions[a,b]

treatment	RP (mV)	OS (mV)	APD$_0$ (ms)	APD$_{40}$ (ms)	APD$_{10}$ (ms)
(A)					
control	−90.8 ± 0.9	18.3 ± 0.7	220 ± 7	405 ± 9	483 ± 12
P U Y	−90.8 ± 0.7	20.8 ± 0.6[c]	311 ± 5[c]	539 ± 6[c]	685 ± 8[c]
hypericin (**1**)	−88.4 ± 0.9	22.2 ± 0.8	388 ± 10[d]	624 ± 12[d]	824 ± 15[d]
(B)					
control	−84.4 ± 0.9	22.8 ± 1.1	190 ± 8	359 ± 5	492 ± 9
FSK	−81.8 ± 0.9	27.4 ± 1.7[c]	244 ± 8[c]	372 ± 4[c]	553 ± 15[c]
hypericin (**1**)	−82.2 ± 0.6	24.1 ± 1.1	232 ± 18	399 ± 11	670 ± 15[d]
(C)					
control	−89.2 ± 0.7	20.3 ± 0.5	199 ± 5	349 ± 5	410 ± 6
staurosporine	−86.8 ± 1.0	20.2 ± 0.7	264 ± 8[c]	433 ± 8[c]	534 ± 12[c]
hypericin (**1**)	−84.6 ± 0.7[d]	17.8 ± 0.4[d]	279 ± 0.9[d]	481 ± 6[d]	632 ± 10[d]

[a] AP were recorded in Ringer Sr²⁺ solution (control), and under various conditions, before and after hypericin (4 μM) application: (A) propanolol (P; 50 μM), urapidil (U; 1 μM), yohimbine (Y; 1 μM); (B) forskolin (FSK, 1 μM); (C) staurosporine (1 μM). [b] RP = resting membrane potential; OS = amplitude of the overshoot; APD$_0$ = duration of the AP measured at 0 mV; APD$_{40}$ and APD$_{10}$ = duration of the AP measured at a membrane potential +40 and +10 mV higher than RP, respectively. The data are means ± SD of 6 different atria. [c] $p > 0.05$, substance vs control. [d] $p > 0.05$, hypericin vs substance.

Table 3. Effects of Hypericin (**1**) on Frog Atrial AP under Various Conditions[a,b]

treatment	RP (mV)	OS (mV)	APD$_0$ (ms)	APD$_{40}$ (ms)	APD$_{10}$ (ms)
(A)					
control	− 87.0 ± 1.0	17.8 ± 0.9	259 ± 10	473 ± 8	567 ± 5
ODQ	− 87.6 ± 0.8	16.3 ± 0.3	274 ± 6	530 ± 7[c]	689 ± 2[c]
hypericin (**1**)	− 87.7 ± 0.5	17.5 ± 0.5	288 ± 6	541 ± 3	689 ± 8
(B)					
control	−92.2 ± 0.8	17.2 ± 0.6	255 ± 7	463 ± 6	557 ± 12
STa	−88.8 ± 1.2	16.0 ± 0.6	234 ± 8	494 ± 7[c]	604 ± 13[c]
hypericin (**1**)	−87.5 ± 0.9	16.5 ± 0.5	321 ± 16[d]	604 ± 13[d]	792 ± 17[d]
(C)					
control	− 93.7 ± 1.0	17.1 ± 0.5	333 ± 16	657 ± 12	793 ± 13
ANF	− 89.8 ± 2.1	16.5 ± 1.0	417 ± 10[c]	800 ± 9[c]	968 ± 15[c]
hypericin (**1**)	− 91.1 ± 1.0	17.5 ± 0.6	497 ± 19[d]	923 ± 11[d]	1152 ± 17[d]

[a] AP were recorded in Ringer Sr²⁺ solution (control) and under various conditions before and after hypericin (4 μM) application: (A) ODQ (13 μM); (B) enterotoxin (STa, 10⁻⁶ U mL⁻¹); (C) ANF (6.5 μM). [b] RP = resting membrane potential; OS = amplitude of the overshoot; APD$_0$ = duration of the AP measured at 0 mV; APD$_{40}$ and APD$_{10}$ = duration of the AP measured at a membrane potential +40 and +10 mV higher than RP, respectively. Each datum represents the means ± SD of 6 different atriums. [c] $p > 0.05$, substance vs control. [d] $p > 0.05$, hypericin (**1**) vs substance.
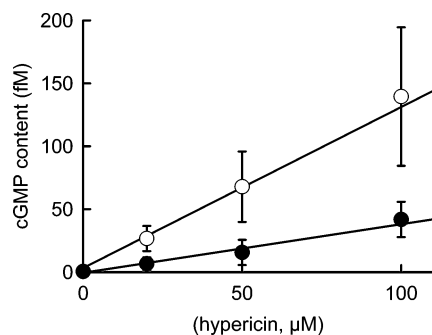

Figure 5. Absolute measurement of the cGMP content of myocytes enzymatically isolated from the frog auricle bathed in Ringer Ca²⁺ solution in the absence (open circles) and in the presence (filled circles) of hypericin (**1**, 4 μM). The regression lines through the points were drawn according to the equations $Y = -0.392 + 1.259X$ in the absence and $Y = -0.465 + 0.386X$ in the presence of hypericin (**1**) (correlation coefficient = 0.99 for both lines), where Y is the cGMP content and X the hypericin (**1**) concentration. The cGMP standards, assayed simultaneously in the absence and presence of hypericin (**1**), were identical excluding a direct artifact in the assay method. Data are means ± SD of 3 auricles.

mean values of their parameters were estimated as individual value of the auricule.[11]

Membrane currents were recorded from single myocytes dispersed by enzymatic digestion of the frog auricle.[12,13] After isolation of the auricle from the heart, the external epithelial sheet surrounding the auricular tissue was carefully detached and removed. The epithelial-free auricle was then pinned at the bottom of an isolation chamber in which the solutions used for the dissociation were maintained at 30 °C and gently stirred with a small magnet. The auricle was successively bathed for 30 min in (i) a Ca²⁺-free Ringer solution; (ii) a Ca²⁺-free Ringer solution containing ethylene glycol tetraacetic acid (EGTA, 0.1 mM); (iii) a Ca²⁺-free Ringer solution; then, (iv) a Ca²⁺-free solution containing 600 mU/mL Type I collagenase (Sigma) and 1.5 mU/mL Type XIV protease (Sigma). All solutions were filtered and oxygenated. When the tissue was digested, the auricle was rinsed twice (10 min) with a Ca²⁺-free Ringer solution and subsequently bathed in a standard Ringer solution and kept at 4 °C. Before experimentation, cells were dispersed by gently shaking the digested auricle in a Petri dish (outer diameter 33 mm, depth 10 mm; Corning, NY) filled with Ringer solution (1 mL). Patch-clamp pipettes (Propper Manufacturing glass, i.d. 1.2 mm, wall 0.2 mm, resistance 1.5 to 2.5 MΩ) were filled with a solution containing the following (mM): KCl, 150; Na2₋creatine phosphate, 5; ATP, 5; EGTA neutralized with KOH, 5; HEPES (KOH) buffer, 10; pH 7.3. The cell current was monitored using an Axopatch feedback amplifier (Axon Instruments, Foster City, CA). Starting from a holding potential (HP) of −80 mV, the membrane potential was displaced in rectangular 10 mV steps at a rate of 0.2 Hz. Positive potentials corresponded to depolarization, and negative currents corresponded to inward cationic currents.[12,13] The amplitude of the ionic current was measured at the peak time; the time to peak (Tp) corresponded to the time needed by the current to reach its maximum value; the time constant of the inactivation phase of the current was obtained by fitting the decay of the falling phase of the current using Acquis 1 software (CNRS, Gif/Yvette, France). Transmembrane potentials and currents were acquired using a Labmaster acquisition card (DMA 100 OEM), driven by Acquis 1 software linked to the mass storage of a desktop computer (AT80486 DX 33), and displayed on an Nicolet 310 oscilloscope (Nicolet, Madison, WI).

Solutions. The composition of the standard Ringer solution was as follows (mM): NaCl, 110.5; CaCl₂, 2; KCl, 2.5; MgCl₂, 1; Na⁺ pyruvate, 5; glucose, 10; HEPES (NaOH) buffer, 10; pH 7.3. The Ca²⁺-free solution, used for cell isolation, was obtained by simple Ca²⁺

removal. Tetrodotoxin (TTX; 0.7 μM) and tetraethylammonium (TEA; 10 mM) were used to entirely inhibit the peak Na$^+$ current (I_{Na}), the delayed outward K$^+$ current (I_K), and to some extent the background inward rectifying K$^+$ current (I_{K1}), respectively. To study the effect of hypericin (**1**) on L-type Ca^{2+} current ($I_{Ca(L)}$), Ca^{2+} was replaced by Sr^{2+} in the control solution. Sr^{2+}, which permeates through L-type Ca^{2+} channels, slows the inactivation of the current ($I_{Sr(L)}$), leading to an increase in APD,[7] and suppresses Ca^{2+}-activated K$^+$ currents (I_{K-Ca})[8] and I_{K1}.[9] Urapidil (Sigma Aldrich Chimie, St Quentin Fallavier, France) and yohimbine (Sigma Aldrich Chimie) were used respectively to inhibit α_1- and α_2-adrenoceptors; propanolol (Sigma Aldrich Chimie) was used to block both β_1- and β_2-adrenoceptors.[11] Adenyl-cyclase (AC) was activated by forskolin (FSK; Calbiochem, La Jolla, CA). Phosphokinases C (PKC) and to a lesser extent A (PKA) were blocked by staurosporine (Sigma Aldrich Chimie). Nitric oxide (NO)-sensitive soluble guanylyl cyclase (sGC) was selectively inhibited by 1*H*-[1,2,4]-oxadiazolo[4,3-*a*]quinoxalin-1-one (ODQ; Sigma Aldrich Chimie). Rat atrial natriuretic peptide (ANP; Sigma Aldrich Chimie) and *Echerichia coli* heat-stable enterotoxin (STa; Sigma Aldrich Chimie) were used to stimulate GC NPR-A receptors and to activate the heat-stable enterotoxin GC receptors, respectively.

Protein Phosphatase 2A (PP-2A) Assay. An eventual effect of hypericin (**1**) on protein phosphatase 2A (PP-2A) was tested using the microscystin bioassay in which PP-2A activity against *p*-nitrophenyl phosphate (pNPP) is determined by quantification of paranitrophenol hydrolyzed from pNPP using absorbance measurements at 405 nm.[14]

NO Synthase-2 (NOS2) Activity Assay. The effect of hypericin (**1**) on NOS2 activity was examined. NO formation was measured by the heme capture method[15] based on the reaction of oxyhemoglobin (HbO$_2$) with NO to form methemoglobin (metHb) and nitrate (HbO$_2$ + NO $\rightarrow$ metHb + NO$_3$). The activity of NOS2 was quantified spectrophotometrically (ϵ = 50 000/M/cm at 401 nm) by absorbance measurements. The reaction was performed in Tris-HCl (pH 7.6) containing L-arginine (1 mM), NADPH (0.1 mM), (6*R*)-5,6,7,8-tetrahydrobiopterin (12 μM; Sigma Aldrich Chimie), (CH$_3$COO)$_2$Mg (1 mM), dithio-L-threitol (300 μM; Sigma Aldrich Chimie), HbO$_2$ (10 μM), and either hypericin (0.1 to 10 μM) or monomethyl-L-arginine (MMA; 1 mM), a competitive inhibitor of NOS2. A stock solution of hypericin (**1**, 10 mM) was prepared in DMSO. Measurements were made in a Safas UV=Mc2 dual-beam spectrophotometer equipped with a thermostated cuvette-holder. NO formation was initiated by rapid addition of a NOS2-containing solution (Cayman Chemicals) and was followed for 10 min at 37 °C. Assay samples were read against blanks containing all components except NOS2. Absorbance between 401 and 411 nm (isobestic point) measures the increase in metHb concentration, which corresponded to the amount of NO generated.

cGMP Immunoassay. A modified cGMP immunoassay was performed on frog auricle myocytes (see below).[16] Frog auricles dissociated by enzymatic digestion were split in two parts, immersed in Petri dishes containing the Ringer Ca^{2+} solution (500 μL), and subsequently weighed. Isobutylmethylxanthine (IBMX, 25 μL; Sigma-Aldrich) was added in one dish (control) at a final concentration of 1 mM. In another dish, IBMX was added together with hypericin (4 μM). The cells were incubated in the dark with mild shaking for 20 min. The cGMP extraction was performed using a commercial kit (RPN 226, Amersham Biosciences) and adapted by adding 55 μL of lysis buffer containing 5% dodecyltrimethylammonium to each dish. After 15 min incubation, aliquots, between 20 and 200 μL in volume, were taken and completed with buffer to a volume up to 500 μL for acetylation. Acetylation of the samples was performed together with cGMP standards varying from 2 to 512 fM per tube. Two cGMP standard series were assayed simultaneously, one of which contained hypericin (**1**, 4 μM). Manufacturer's instructions were followed for the immunoreaction in a 96-well plate, and the absorbance was measured at 450 nm, corresponding to cGMP produced during incubation with hypericin since addition of IBMX inhibits phosphodiesterase, thus avoiding loss of cGMP.

Statistical Analysis. Numerical data are expressed as means $\pm$ SD of *n* preparations tested. Comparison between values were done using the Student's *t* test delivered by the software Sigmaplot (Jandel Scientific GmbH, Erkrath, Germany); *p* values of less than 0.05 were considered significant.

References and Notes

(1) Cardellina, J. H., II. *J. Nat. Prod.* **2002**, *65*, 1073−1084.
(2) Colas, A.; Sauviat, M.-P. In *Rencontres en Toxinologie: Toxines et Recherches Biomédicales*; Goudey-Perriere, F., Bon, C., Puiseux-Dao, S., Sauviat, M.-P., Eds.; Editions Scientifiques et Médicales Elsevier: Paris, 2002; pp 153−166.
(3) Thomas, C.; Pardini, R. S. *Photochem. Photobiol.* **1992**, *55*, 831−837.
(4) Miskovsky, P.; Sureau, F.; Chinsky, L.; Turpin, P. Y. *Photochem. Photobiol.* **1995**, *62*, 546−549.
(5) Siepmann, M.; Krause, S.; Joraschky, P.; Mück-Weymann, M.; Kirch, W. *Br. J. Clin. Pharmacol.* **2002**, *54*, 277−282.
(6) Kubin, A.; Alth, G.; Jindra, R.; Jessner, G.; Ebermann, R. *Photochem. Photobiol.* **1996**, *36*, 103−108.
(7) Chesnais, J.-M.; Sauviat, M.-P.; Vassas, J.-M. *J. Physiol.* (*Paris*) **1969**, *61*, 244.
(8) Coraboeuf, E.; Carmeliet, E. *Pflügers Arch.* **1982**, *392*, 352−359.
(9) Shioya, T.; Matsuda, H.; Noma, A. *Pflügers Arch.* **1993**, *422*, 427−435.
(10) Sauviat, M.-P.; Garnier, P.; Goudey-Perriere, F.; Perriere, C. *Toxicon* **1995**, *33*, 1207−1213.
(11) Sauviat, M.-P.; Marquais, M.; Vernoux, J.-P. *Toxicon* **2002**, *40*, 1155−1163.
(12) Sauviat, M.-P.; Colas, A.; Pages, N. *BMC Pharmacol.* **2002**, *2*, 15.
(13) Sauviat, M.-P.; Vercauteren, J.; Grimaud, N.; Jugé, M.; Nabil, M.; Petit, J.-Y.; Biard, J.-F. *J. Nat. Prod.* **2006**, *69*, 559−562.
(14) Rivasseau, C.; Racaud, P.; Deguin, A.; Hennion, M.-C. *Anal. Chim. Acta* **1999**, *394*, 243−257.
(15) Feelisch, M.; Kubitzek, D.; Werringloer, J. In *Methods in Nitric Oxide Research*; Feelisch, M.; Stamler, J. S., Eds.; John Wiley & Sons, Ltd: Chichester, UK, 1996; pp 455−478.
(16) Negrerie, M.; Bouzhir, L.; Martin, J.-L.; Liebl, U. *J. Biol. Chem.* **2001**, *276*, 46815−46821.
(17) Chesnais, J.-M.; Coraboeuf, E.; Sauviat, M.-P.; Vassas, J.-M. *C. R. Acad. Sci.* **1969**, *273*, 204−207.
(18) Dittrich, M.; Jurevicius, J.; Georget, M.; Rochais, F.; Fleischmann, B. K.; Hescheler, J.; Fischmeister, R. *J. Physiol.* **2001**, *534*, 109−121.
(19) Gallo, M. P.; Malan, D.; Bedendi, I.; Biasin, C.; Alloatti, G.; Levi, R. C. *Pflügers Arch.* **2001**, *441*, 621−628.
(20) Wang, Y. G.; Rechenmacher, C.; Lipsius, S. L. *J. Gen. Physiol.* **1998**, *11*, 113−125.
(21) Shen, J. B.; Pappano, A. J. *J. Pharmacol. Exp. Ther.* **2002**, *301*, 501−506.